Biophysical Chemistry 254 (2019) 106262

Contents lists available at ScienceDirect

Biophysical Chemistry

journal homepage: www.elsevier.com/locate/biophyschem

Research Article

Label-free, real-time on-chip sensing of living cells via grating-coupled surface plasmon resonance

Giulia Borile[a,b,*], Stefano Rossi[a,b,1], Andrea Filippi[a,b,c,1], Enrico Gazzola[b], Pietro Capaldo[b,d], Claudia Tregnago[e], Martina Pigazzi[a,e], Filippo Romanato[a,b,d,f]

[a] Fondazione Institute of Pediatric Research Città della Speranza, Corso Stati Uniti 4, 35127 Padua, Italy
[b] Department of Physics and Astronomy "G. Galilei", University of Padua, Via Marzolo 8, 35131 Padua, Italy
[c] Fondazione Bruno Kessler, Via Sommarive 18, 38123 Trento, Italy
[d] CNR-INFM TASC IOM National Laboratory, Area Science Park S.S, 14 km 163.5, 34012 Trieste, Italy
[e] Women and Child Health Department, Haematology-Oncology Clinic and Lab, University of Padua, Via Giustiniani 3, 35128 Padua, Italy
[f] Laboratory for Nanofabrication of Nanodevices, Corso Stati Uniti 4, 35127 Padua, Italy

HIGHLIGHTS

- Surface Plasmon Resonance (SPR) keeps moving from biochemistry to cell biology.
- Grating-coupled SPR is amenable for integration in microfluidic chamber.
- Grating-coupled SPR has been successfully used for live cell investigation.

GRAPHICAL ABSTRACT

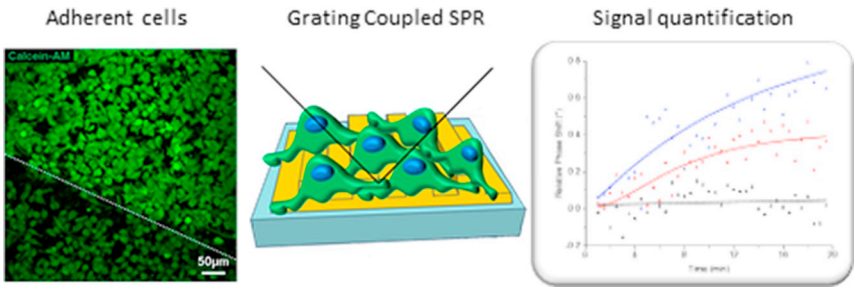

ARTICLE INFO

Keywords:
Surface plasmon resonance
Grating
Nanostructure
Live cells

ABSTRACT

The application of nanotechnologies to address biomedical questions is a key strategy for innovation in biomedical research. Among others, a key point consists in the availability of nanotechnologies for monitoring cellular processes in a real-time and label-free approach. Here, we focused on a grating-coupled Surface Plasmon Resonance (GC-SPR) sensor exploiting phase interrogation. This sensor can be integrated in a microfluidic chamber that ensures cell viability and avoids cell stress. We report the calibration of the sensor response as a function of cell number and its application to monitor cell adhesion kinetics as well as cell response to an external stimulus. Our results show that GC-SPR sensors can offer a valuable alternative to prism-coupled or imaging SPR devices, amenable for microfluidic implementation.

1. Introduction

Biomedical research is continuously evolving and the need for more sophisticated and innovative tools is rising mainly due to the contamination of different knowledge.

Cell-based analysis constitutes a fundamental step in life science research, where it is used to assess cell behaviour and response to external stimuli [1]. A gold standard approach to visualize cell response is

Abbreviations: SPR, surface plasmon resonance; GC, grating coupled

* Corresponding author at: Fondazione Institute of Pediatric Research Città della Speranza, Corso Stati Uniti 4, 35127 Padua, Italy.
E-mail address: giulia.borile@unipd.it (G. Borile).

[1] Contributed equally.

https://doi.org/10.1016/j.bpc.2019.106262
Received 18 June 2019; Received in revised form 28 August 2019; Accepted 2 September 2019
Available online 03 September 2019
0301-4622/

offered by fluorescence microscopy, which usually requires cell labelling and post-detection analysis, this latter causing the complete loss of information about the kinetic of the process [2]. Moreover, cell adhesion to specific substrates is of increasing interest in the field of 3D culture models aiming to recapitulate in vivo complexity with the ease of in vitro culture [3].

Surface Plasmon Resonance (SPR) based sensors are of growing interest because of the promising label- and enzyme-free, as well as real-time detection approach for the biological specimens [4,5].

SPR refers to the collective oscillation of conduction electrons at the interface between a conductor material (typically gold or silver) and a dielectric (i.e. air or water, but also nucleic acids or proteins) upon light interaction [6]. Nanostructured plasmonic biosensors have been developed to improve miniaturization, integration and multiplexing in a lab-on-a-chip approach, while providing high sensitivity and specificity [7,8].

SPR biosensing is widely used to investigate the binding affinity and dynamics of two ligands and has been successfully applied to immunoassays demonstrating the suitability of the technique for molecular biology studies [9,10]. It allows monitoring molecular interactions occurring within the first few hundreds of nm over a gold surface, thanks to the plasmon evanescent field, that exponentially decays as it penetrates the material [6].

There are two major classes of SPR coupling technique that are based, respectively, on prism- and grating-coupling. In the first configuration, the light is totally reflected at the interface between the prism and the thin metal layer, making it particularly suitable for SPR sensing and the most used in commercial systems [4]. The interrogation system is usually based on angular interrogation, but some systems work through intensity modulation, the so-called SPR-imaging [11,12]. However, the recent interest in lab-on-a-chip brought the need for further integration of the SPR sensors, which is difficult to obtain with prism-coupling, because of the cumbersome optical system required for measurement. Grating-coupled SPR (GC-SPR) utilizes a metallic nanofabricated grating combined with excitation and detection system azimuthally rotated, that has been shown to reach performances close to prism-coupled systems [13,14]. In this configuration, the sensitivity of the resonance to incident light polarization allows an approach called “phase-interrogation”, which minimize moving parts during the scan. The system used in this work has been previously optimized for phase-interrogation in water-based environment [14,15]. This approach was found to be particularly suitable for integration of the plasmonic sensor in microfluidic Polydimethylsiloxane (PDMS) circuits, to allow sensing procedures and tightly control volumes, including multiplexing [7,16].

Recently, applications of SPR sensors have been reported for dynamic cellular analysis exploiting their label-free and real-time approach, with promising results [17]–[19]. Although most applications to cell biology are based on SPR imaging [10,20], live cell dynamic reactions to chemical stimuli are detectable as a change of the angle of resonance. Thanks to the spatial confinement of the evanescent optical field, SPR sensing ensures the precise monitoring of phenomena occurring on the cell membrane (like adhesion or rearrangement), regardless of changes in the intracellular compartments, that are far from the SPR sensitive volume. To date, several challenges need to be addressed to promote the application of SPR-based label-free cell analyses, such as the maintenance of cell integrity during the experimental process [9,17,21]. Most of commercially available instruments use glass slides coated with gold, that should be installed on the prism before analysis with a careful handling process to reduce cell damage [17]. Moreover, some instruments can tolerate in the microfluidic components only particulates under few microns, thus cells would cause clogging [17].

Here, we performed an experimental application of our GC-SPR integrated in a PDMS microfluidic chamber to label-free monitor cell adhesion capability and cell-surface interaction, while scaling down medium volume and maintaining cell integrity during manipulation. For this study we focused on SHI-1, a human acute myeloid leukemia (AML) cell line, that in vitro grows in suspension. Although this is a highly specific cell line, most of the results can be transferred to any other cell type as will be discussed. We used this cell line in the context of a wider research project aimed at evaluating the role of the bone marrow microenvironment on leukemia cells [22]. Indeed, in vivo AML cells home to the bone marrow, where they interact with stroma components and extracellular matrix proteins [23,24]. AML cells derive their proliferative capacity from this interaction and the following adhesion. The method we show here poses the basis for further in vitro studies of cell adhesion dynamics and affinity to different substrates, that currently rely mainly on microscopy-based analysis.

2. Materials and methods

2.1. Numerical simulations

We performed numerical simulations using the commercial software COMSOL Multiphysics® [25]. The design of the structure replicates the physical dimensions of the grating (duty cycle, linewidth and height) and the field is simulated at a fixed azimuth (as done experimentally) at the resonance angle. Both gold and medium are considered bulk. The same simulation was performed using two refractive indexes: 1.33 for water and 1.38 for cells. The colour code adopted to visualize the field represents in red the skin depth.

2.2. Plasmonic grating fabrication and PDMS embedding

Grating fabrication was performed as previously described by our group [15]. Briefly, digital gold gratings were fabricated, choosing a period of 400 nm and a linewidth of 200 nm, corresponding to a duty cycle of 50%. To fabricate the plasmonic gratings a positive photoresist, Microposit S1805®, was chosen for the laser interference lithography (LIL) [16]. LIL optimal dose was found to be 65 mJ/cm^2, corresponding to exposure times around 10 min. A 24° incidence angle was used to fabricate gratings with a period of 400 nm, according to the optimization provided in [15]. The grating morphology was characterized by Atomic Force Microscopy. Microfluidic chambers were realized in PDMS with soft lithography and covalently bonded on the SPR chip, as previously described [14].

2.3. GC-SPR detection and analysis setup

For SPR generation and detection, we used a custom-made bench setup based on phase interrogation, previously adopted for other applications [14]. Briefly, an incident laser beam at 633 nm crosses a half-wave plate mounted on a motorized rotation system, before reaching the sensor. Reflected light is collected by a CMOS camera and the entire system is controlled by a custom-made software. The recorded reflectance is a function of the polarization angle and it is therefore fitted with a harmonic function. A shift of the function phase angle is proportional to the refraction index variation [17].

2.4. Cell culture

SHI-1 cells (purchased from DSMZ, Germany) were maintained in DMEM supplemented with 10% FBS at 37 °C and 5% CO_2. Prior to the experiments, sensors were coated with Fibronectin (20 mg/mL in Hank's Balances Salts Solution, HBSS) for 2 h. After two washouts with HBSS, cells were seeded at the desired concentration.

2.5. Cell viability staining

SHI-1 cells were let adhere to the surface, then washed twice in PBS to remove non-adherent cells and debris. To identify cells and evaluate their viability, Calcein-AM (ThemoFisher) was used following manufacturer's instructions.

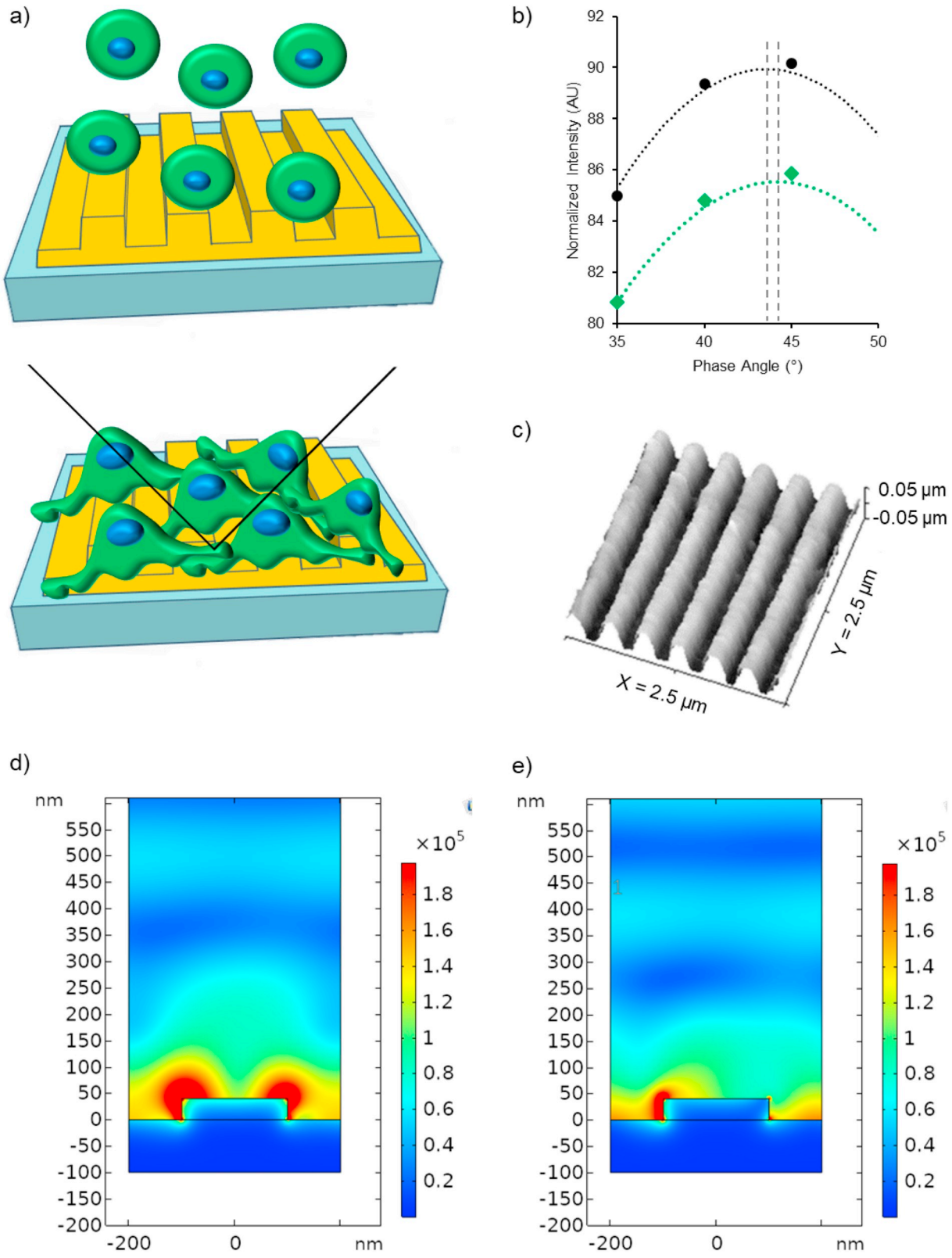

Fig. 1. a) Representation of the experimental approach used to interrogate cell adhesion with GC-SPR. Cells in suspension (top) adhere to the gold grating (bottom). Black line indicates the incident light path and the reflected light path used to detect signal. b) Details of polarization spectra acquired in no cell condition (black) and with cells adherent to the surface (green). The gray lines indicate the spectra maximum, calculated interpolating experimental data (points) to a sinusoidal curve (dotted line). c) Grating morphology reconstructed by Atomic Force Microscopy. d) COMSOL simulations of the field over the grating in water and (e) in a medium with cell refractive index (1.38). (For interpretation of the references to colour in this figure legend, the reader is referred to the web version of this article.)

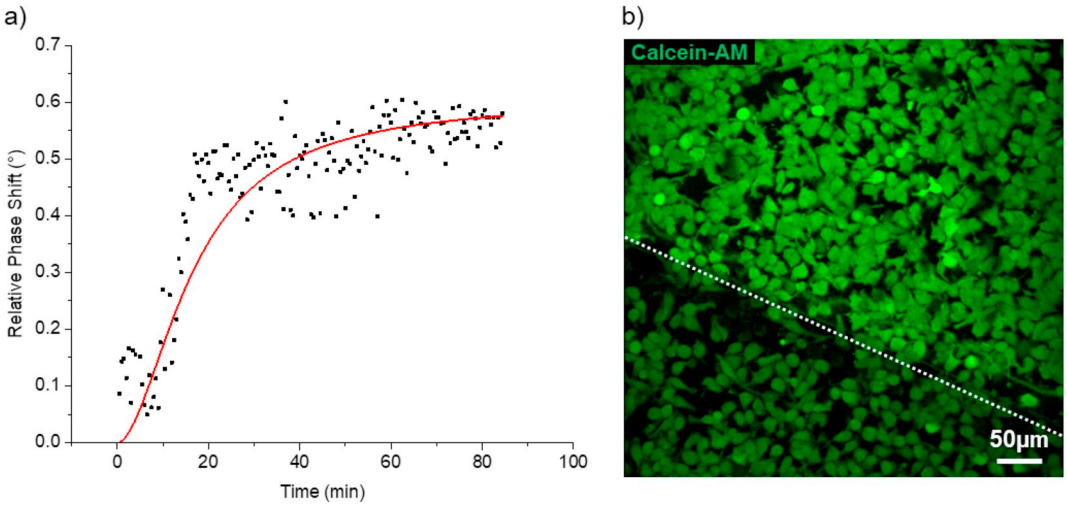

Fig. 2. a) Fibronectin coating on gold grating monitored as SPR phase angle variation in the microfluidic chamber. Representative data of one out of three different experimental replicates, in red Hill fit: $R^2 = 0.98$. b) SHI-1 cancer cells after seeding on fibronectin coating, imaged at the interface between the regions where the substrate is either glass (below the dotted line) or gold grating (over the dotted line). Calcein-AM staining of living cells did not highlight differences between the two surfaces, nor differences were observed in the cell shape as quantified in the results section. $Area_{Gold}$: 214 ± 8 µm^2 vs. $Area_{Glass}$: 195 ± 7 µm^2; $AspectRatio_{Gold}$: 1.57 ± 0.07, vs. $AspectRatio_{Glass}$: 1.58 ± 0.08; $Roundness_{Gold}$: 0.67 ± 0.02, vs. $Roundness_{Glass}$: 0.68 ± 0.03; $n = 50$ cells per condition, *t*-test not significant). (For interpretation of the references to colour in this figure legend, the reader is referred to the web version of this article.)

2.6. Live imaging with 2-photon microscope

For live cell imaging we used a custom-build 2-photon microscope, previously described by our group for different applications [26]. Briefly, excitation wavelength was set at 800 nm and Calcein-AM emission was imaged with a 525/40 nm bandpass filter. Images were processed and analyzed with FIJI software. All data are reported as mean ± s.e.m. (standard error of the mean).

3. Results and discussion

3.1. GC-SPR in conical mounting characterization

The system used in this work has been developed by our group and optimized for water-based environment. Briefly, the sensitive area consists of a gold nano-grating embedded in a PDMS circuit positioned on a rotating stage. The adoption of azimuthal rotation of the grating with respect to the incidence plane (see representation in Fig. 1a) allowed to obtain the best performances. Incident light crosses a rotating half-wave plate, and this is the only moving part during the scan, thus making the system alignment simpler than traditional setups where the light source and detector need to move accordingly. In this configuration, reflectance exhibits a sinusoidal dependence as a function of light polarization angle [15] that is acquired and fitted as in Fig. 1b. A change of the refractive index over the grating causes a shift in the reflectance spectra (Fig. 1b) whose fitting allows to identify the maximum of the curve. This angular shift is proportional to the refractive index variation with a sensitivity up to 300°/RIU as was previously estimated by our group [15].

SPR performance relies on fabrication parameters, that were previously identified in 400 nm period and 40 nm line depth in aqueous medium [15]. Thus, morphological analysis of the fabricated samples was performed by Atomic Force Microscopy (see Fig. 1c). The obtained profiles revealed a good agreement between the fabricated grating and the theoretical parameters. All the gratings used for the experiments reported in this paper were tested for fabrication parameters.

Then, we aimed to evaluate the penetration depth of the field into a biological material. To reach this goal we used the COMSOL Multiphysics® software. It allows to design the desired structure, where materials are represented by their complex permittivity, and exploit a Finite Elements Method to solve its interaction with incident light [17]. Since cells are big with respect to the nanostructure scale, they were treated as a bulk. In this way, we could achieve information about the surface plasmon evanescent field shape and penetration in the cell. The skin depth, visualized in red in Fig. 1d and e, is well below 100 nm in water and even less in a medium with the estimated average refractive index of a cell. This means that the large part of plasmonic field probes the cell plasma membrane, that constitutes the first 10 nm over the adhesion layer [2]. This aspect is crucial, since it allows to monitor changes in the adhesion of cells over the gold surface, independently of rearrangements occurring inside the cell cytosol, that is too far from the sensitive volume. In comparison with optical microscopy techniques, this confinement of the acquired signal to the first layers over the grating makes the system intrinsically "confocal", and the data obtained belong to an "optical section" of around 1% of the cell height.

3.2. Fibronectin coating as adhesion layer and anti-fouling agent

SHI-1 is a bone marrow (BM)-derived myeloid leukemia cell line that grows in suspension but can adhere to surfaces upon a coating with proteins typical of the extracellular matrix. We identified the fibronectin, that in its soluble form is highly present in blood plasma and is one of the components of the extracellular matrix, a good coating substrate to promote cell adhesion. The most effective adhesion coating resulted in fibronectin at a concentration of 20 mg/mL for 2 h. Lower concentration did not ensure stable and reproducible cell adhesion, leading to cell detachment only with medium flux, whereas with higher concentrations we did not observe an increase in cell adhesion stability. We thus monitored with our GC-SPR system the coverage of the sensitive area with fibronectin that reached a steady state after 80 min with a sigmoid curve, as expected (Fig. 2a, representative data of three different experimental replicates, Hill fit: $R^2 = 0.98$). Interestingly, we observed that fibronectin coating acted as an anti-fouling agent. This effect is important since it avoids any other interfering agent being adsorbed to the grating or involved in any reaction. This is of crucial relevance while doing experiments with viable cells considering that their growth medium is full of salts, proteins and vesicles coming both from the cells themselves and from serum added to culture medium. To assess whether SHI-1 cells could be affected by the gold grating, we stained cells with Calcein-AM, a standard indicator that becomes

fluorescent only in viable cells. A representative image of cells loaded with Calcein-AM and acquired at the interface between gold and glass, is shown in Fig. 2b. Regardless of the substrate, cells accumulated Calcein-AM and showed fluorescent signal that appears stronger on the gold substrate because of reflection. In three experimental replicates we acquired random fields of fluorescent cells and compared cell area (Gold: 214 ± 8 μm^2 vs. Glass: 195 ± 7 μm^2, n = 50 cells per condition, t-test not significant, p-value = .1) that did not show significant differences between the two substrates. Then we wanted to compare cell morphology using standard shape descriptors like Aspect Ratio (Gold: 1.57 ± 0.07, vs. Glass: 1.58 ± 0.08, n = 50 cells per condition, t-test not significant, p-value = .9) and Roundness (Gold: 0.67 ± 0.02, vs. Glass: 0.68 ± 0.03, n = 50 cells per condition, t-test not significant, p-value = .8) and even this analysis did not revealed significant differences. Thus, the gold grating does not affect SHI-1 cells adhesion or viability.

3.3. GC-SPR label-free quantification of adherent cells

SHI-1 cells were then used to monitor and quantify cell adhesion to the selected coating. The adhesion of SHI-1 cells over the fibronectin-coated gold grating causes a large shift in the phase angle proportional to the surface coverage, that is correlated to number of adherent cells. Using different cell concentrations, it was possible to build a calibration scale of the SPR response of our system (Fig. 3a representative trace from single experiments, Fig. 3b mean value and s.e.m. of three experimental replicates). The minimum detectable number of cells (limit of detection) corresponded to around 100 cells/mm^2, while the maximum phase shift (sensor saturation) was registered for numbers over 2000 cells/mm^2 (Δα = 0.91° ± 0.02°). This last parameter is in good agreement with a similar experiment where authors reported that saturation was reached with 1600 cells/mm^2 in a prism-coupled SPR device (ΔR = 0.78°) [18]. In this work, the authors adopted a commercial prism-coupled device and calibrated the system elucidating the relationship between the cell number and the change in the angle of resonance (ΔR) up to its maximum variation. While the two systems adopt different strategies to test whole cell number over the sensitive area, we can compare the angular change in function of the cell number over the surface that for the prism-coupled system is reported to be 0.00044°/ (cells/mm^2) [18] while in our system is 0.00045°/(cells/mm^2). This comparison between prism-coupled and grating-coupled system is commonly adopted to assess home-made systems compared to commercial ones. Thus, a GC-SPR system with phase interrogation can offer an alternative approach to whole cell adhesion experiments, in addition to prism coupled-systems.

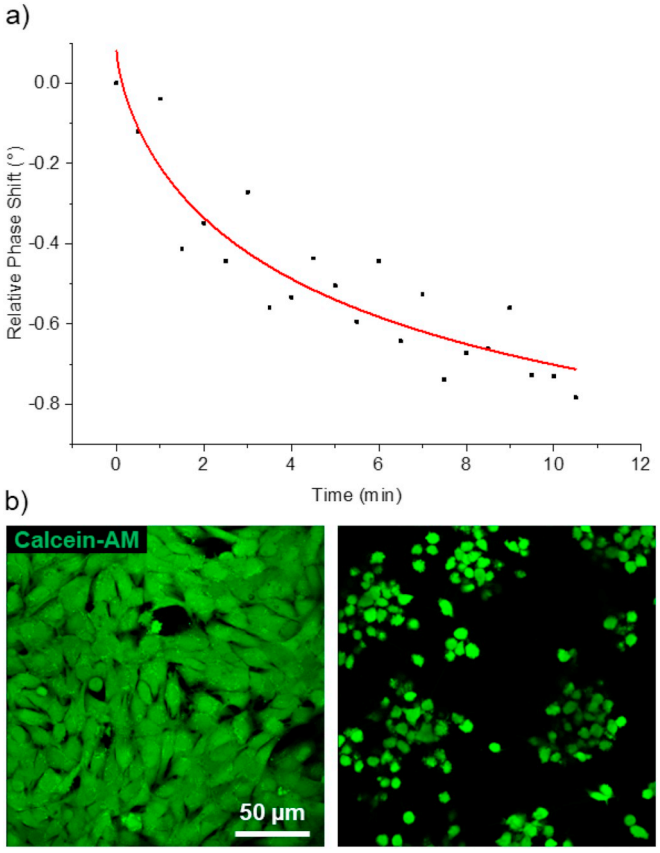

Fig. 4. a) SHI-1 cancer cells were treated with trypsin to detach them from grating. As cells detach from the sensing surface, a reduction in SPR signal can be observed. Red curve represents an exponential fit of the data. The curve is representative of three experimental replicates. b) Representative images of cells loaded with Calcein-AM before (left) and after (right) trypsin administration, respectively. (For interpretation of the references to colour in this figure legend, the reader is referred to the web version of this article.)

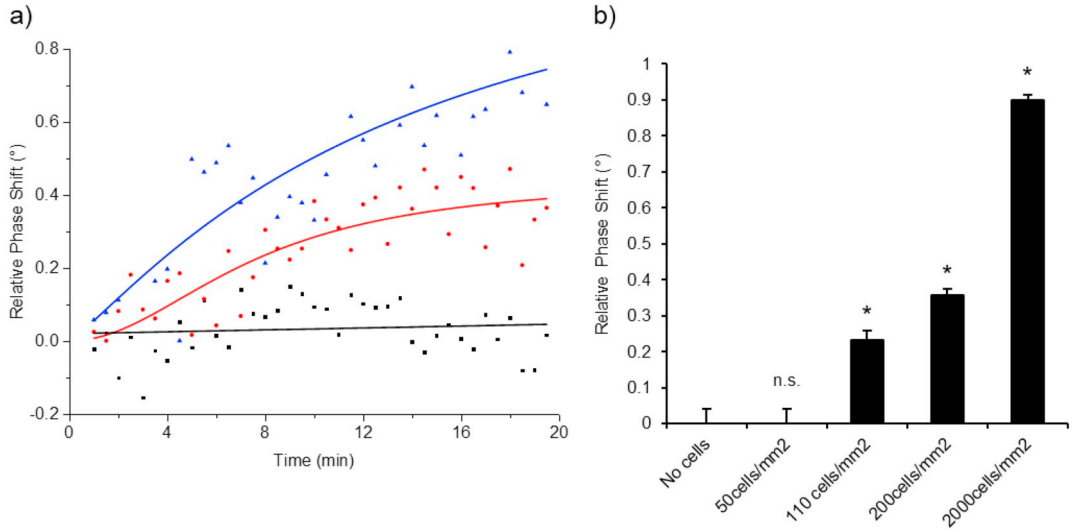

Fig. 3. a) SHI-1 cancer cells were monitored during adhesion to coated gratings at room temperature. Black dots represent cell medium signal, red dots represent the final concentration of 200cells/mm^2 and blue dots 2000cells/mm^2. SPR phase spectra were acquired every 10 s. Phase shift (with respect to baseline) was calculated with a custom MatLab® routine, then fitted with a Hill function. b) Calibration of the SPR response as a function of cell concentration. Histogram bars represent the mean ± s.e.m. of at least three experimental replicates. t-test was performed comparing with no cell condition: * means p-value < .05, n.s. means not significant. (For interpretation of the references to colour in this figure legend, the reader is referred to the web version of this article.)

3.4. GC-SPR label-free real-time monitoring of cell detachment

To further confirm that SPR can detect morphological changes of cells, we challenged adherent cells with trypsin, an enzyme that causes structural shrinking and detachment from the fibronectin coating. The SPR response resulted in a $\Delta\alpha = -0.72^{\circ}$ consisting in a reduction of the cell membrane-covered surface around 95%, consistent with the microscopy analysis performed by fluorescence imaging (see Fig. 4). This approach opens to further investigation aimed at evaluating the effect of adhesion properties in response to drug stimulation since detachment of leukemia cells from extracellular matrix may improve the outcome of chemotherapy.

4. Conclusions

In this proof-of-principle paper we have shown that grating-coupled SPR biosensors can be used for live cell dynamics investigation. Our GC-SPR system is based on phase interrogation, that means a sinusoidal behavior of the reflectance as a function of incident light polarization. The SPR signal, in terms of phase shift, is proportional to the surface coverage over the grating, allowing a calibration for cell number quantification.

Most of the applications of SPR to whole cell studies relies on SPR imaging approaches. Indeed, in SPR imaging, signal results from amplitude modulation at a fixed angle, unlike GC-SPR or PC-SPR where a phase or polar angle scan is performed. Because they are based on intensity interrogation, SPR imaging sensors suffer from worse performance with respect to angle scanning systems ([12] and for a complete review see [9]). Comparing the GC-SPR approach to the more diffused PC-SPR, we can highlight some advantages and disadvantages. The major advantages ofGC-SPR technique are mainly the simple setup configuration with a single moving part during the scan (the rotating half-wave plate) and the sensitive area (gold grating) amenable for integration in a PDMS circuit that maximizes cell viability and reduces stresses. As discussed in the results section, the performance obtained in terms of cell number is comparable to a commercially available prism-coupled device. Moreover, the possibility of grating fabrication with imprinting technique is suitable for large number production [16].

On the other hand, we recognize two disadvantages: the poor spreading of such systems from a commercial point-of-view leads to slower implementation and engineering of the technique. Then, we experienced that some cell types (for example fibroblasts) are sensitive to the grating structure, not in terms of viability but cell shape [3]. Indeed, we observed that fibroblasts seeded on gold grating aligned along the grating direction and assumed a “rectangular-like” shape, that was much different from the same cell shape on glass or planar gold. This phenomenon is well known and sometimes exploited to challenge cell membrane, but it can be not convenient for all experiments [27].

In conclusion, our methodological approach results in good resolution, compact, inexpensive and very simple cell detection setup, and opens for further research strategies based on the integration of the sensitive grating into a microfluidic chamber that could improve cell biology studies.

Acknowledgement

G.B. acknowledges the support from Fondazione Istituto di Ricerca Pediatrica (Grant: MyFirstIRP 19/06IRP). The authors declare no conflict of interest.

References

[1] S. Lindström, Flow cytometry and microscopy as means of studying single cells: a short introductional overview, Methods Mol. Biol. 853 (2012) 13–15.
[2] B. Soediono, Alberts - Molecular Biology of the Cell, (1989).
[3] I.O. Doagă, T. Savopol, M. Neagu, A. Neagu, E. Kovács, The kinetics of cell adhesion to solid scaffolds: an experimental and theoretical approach, J. Biol. Phys. 34 (5) (2008) 495–509.
[4] X. Wang, S. Zhan, Z. Huang, X. Hong, Review: advances and applications of surface plasmon resonance biosensing instrumentation, Instrum. Sci. Technol. 41 (6) (2013).
[5] F.S. Ligler, Perspective on optical biosensors and integrated sensor systems, Anal. Chem. 81 (2) (2009) 519–526.
[6] W.L. Barnes, Surface plasmon-polariton length scales: a route to sub-wavelength optics, J. Opt. A Pure Appl. Opt. 8 (2006) S87.
[7] E. Ouellet, C. Lausted, T. Lin, C.W.T. Yang, L. Hood, E.T. Lagally, Parallel microfluidic surface plasmon resonance imaging arrays, Lab Chip 10 (2010) 581–588.
[8] D.S. Wang, S.K. Fan, Microfluidic surface plasmon resonance sensors: from principles to point-of-care applications, Sensors (Switzerland) 16 (8) (2016).
[9] R.B.M. Schasfoort, F. Abali, I. Stojanovic, G. Vidarsson, L.W.M.M. Terstappen, Trends in SPR cytometry: advances in label-free detection of cell parameters, Biosensors 8 (4) (2018).
[10] I. Stojanović, R.B.M. Schasfoort, L.W.M.M. Terstappen, Analysis of cell surface antigens by surface plasmon resonance imaging, Biosens. Bioelectron. 52 (2014) 36–43.
[11] H.H. Nguyen, J. Park, S. Kang, M. Kim, Surface plasmon resonance: a versatile technique for biosensor applications, Sensors (Switzerland) 15 (5) (2015) 10481–10510.
[12] M. Puiu, C. Bala, SPR and SPR imaging: recent trends in developing nanodevices for detection and real-time monitoringof biomolecular events, Sensors (Switzerland) 16 (6) (2016).
[13] G. Ruffato, et al., Implementation and testing of a compact and high-resolution sensing device based on grating-coupled surface plasmon resonance with polarization modulation, Sensors Actuators B Chem. 185 (2013) 179–187.
[14] A. Sonato, et al., A surface acoustic wave (SAW)-enhanced grating-coupling phase-interrogation surface plasmon resonance (SPR) microfluidic biosensor, Lab Chip 16 (7) (2016) 1224–1233.
[15] S. Rossi, E. Gazzola, P. Capaldo, G. Borile, F. Romanato, Grating-coupled surface plasmon resonance (GC-SPR) optimization for phase-interrogation biosensing in a microfluidic chamber, Sensors (Switzerland) 18 (5) (2018) 1621.
[16] E. Gazzola, A. Pozzato, G. Ruffato, E. Sovernigo, A. Sonato, High-throughput fabrication and calibration of compact high-sensitivity plasmonic lab-on-chip for biosensing, Optofluidics, Microfluid. Nanofluidics 3 (1) (2016) 13–21.
[17] E. Zeidan, C.L. Kepley, C. Sayes, M.G. Sandros, Surface plasmon resonance: a label-free tool for cellular analysis, Nanomedicine 10 (11) (2015) 1833–1846.
[18] Y. Yanase, H. Suzuki, T. Tsutsui, T. Hiragun, Y. Kameyoshi, M. Hide, The SPR signal in living cells reflects changes other than the area of adhesion and the formation of cell constructions, Biosens. Bioelectron. 22 (6) (2007) 1081–1086.
[19] H. Etayash, K. Jiang, S. Azmi, T. Thundat, K. Kaur, Real-time detection of breast cancer cells using peptide-functionalized microcantilever arrays, Sci. Rep. 5 (2015) 13967.
[20] A. Mendoza, D.M. Torrisi, S. Sell, N.C. Cady, D.A. Lawrence, Grating coupled SPR microarray analysis of proteins and cells in blood from mice with breast cancer, Analyst 141 (2016) 704–712.
[21] A.R. Ferhan, J.A. Jackman, J.H. Park, N.J. Cho, D.H. Kim, Nanoplasmonic sensors for detecting circulating cancer biomarkers, Adv. Drug Deliv. Rev. 125 (2018) 48–77.
[22] G. Borella, et al., Development of innovative preclinical in vitro and in vivo tools for an effective Therapeutic strategy in pediatric acute myeloid leukemia, 3rd ESH Scientific Workshop on Haematological Tumour Microenvironment And Its Therapeutic Targeting, 2019.
[23] P.S. Becker, Dependence of acute myeloid leukemia on adhesion within the bone marrow microenvironment, The Scient. World J. 2012 (2012) 856467.
[24] A. Gruszka, D. Valli, C. Restelli, M. Alcalay, Adhesion deregulation in acute myeloid leukaemia, Cells 8 (1) (2019) 66.
[25] G. Parisi, P. Zilio, F. Romanato, Complex Bloch-modes calculation of plasmonic crystal slabs by means of finite elements method, Opt. Express 20 (15) (2012) 16690–16703.
[26] A. Filippi, et al., Multimodal label-free ex vivo imaging using a dual-wavelength microscope with axial chromatic aberration compensation, J. Biomed. Opt. 23 (9) (2018).
[27] K. Lee, et al., Contribution of actin filaments and microtubules to cell elongation and alignment depends on the grating depth of microgratings, J. Nanobiotechnol. 14 (1) (2016) 35.